

Optical polarization properties of a nanowire quantum dot probed along perpendicular orientations

Gabriele Bulgarini, Michael E. Reimer, and Val Zwiller

Citation: *Appl. Phys. Lett.* **101**, 111112 (2012); doi: 10.1063/1.4752453

View online: <http://dx.doi.org/10.1063/1.4752453>

View Table of Contents: <http://apl.aip.org/resource/1/APPLAB/v101/i11>

Published by the [American Institute of Physics](#).

Related Articles

Synthesis and upconversion luminescence of N-doped graphene quantum dots

Appl. Phys. Lett. **101**, 103107 (2012)

Single photon emission in the red spectral range from a GaAs-based self-assembled quantum dot

Appl. Phys. Lett. **101**, 103108 (2012)

Enhancement of spontaneous emission in three-dimensional low refractive-index photonic crystals with designed defects

Appl. Phys. Lett. **101**, 071109 (2012)

Optical properties and effect of carrier tunnelling in CdSe colloidal quantum dots: A comparative study with different ligands

AIP Advances **2**, 032132 (2012)

Controlling the photoluminescence of acceptor and donor quantum dots embedded in a nonlinear photonic crystal

Appl. Phys. Lett. **101**, 051115 (2012)

Additional information on *Appl. Phys. Lett.*

Journal Homepage: <http://apl.aip.org/>

Journal Information: http://apl.aip.org/about/about_the_journal

Top downloads: http://apl.aip.org/features/most_downloaded

Information for Authors: <http://apl.aip.org/authors>

ADVERTISEMENT



HAVE YOU HEARD?

Employers hiring scientists
and engineers trust
physicstodayJOBS



<http://careers.physicstoday.org/post.cfm>

Optical polarization properties of a nanowire quantum dot probed along perpendicular orientations

Gabriele Bulgarini,^{a)} Michael E. Reimer, and Val Zwiller
Kavli Institute of Nanoscience, Delft University of Technology, The Netherlands

(Received 22 March 2012; accepted 30 August 2012; published online 14 September 2012)

We report on the optical properties of single quantum dots in nanowires probed along orthogonal directions. We address the same quantum dot from either the nanowire side or along the nanowire axis via reflection on a micro-prism. The collected photoluminescence intensity from nanowires lying on a substrate is improved 3-fold using the prism as compared to usual collection from the top. More importantly, we circumvent the polarizing effect of the nanowire and access the intrinsic polarization properties of the quantum emitter. Our technique is compatible with the design of complex nanowire devices for the development of quantum opto-electronics. © 2012 American Institute of Physics. [<http://dx.doi.org/10.1063/1.4752453>]

The polarization state of photons is of fundamental importance in the field of quantum information and for the development of future quantum opto-electronic devices. For example, polarization-entangled photons are employed in quantum cryptography for secure communication¹ or necessary in the future implementations of a quantum repeater.² In this prospect, quantum dots grown in nanowires are ideal candidates for entangled photon generation due to the high symmetry provided by the nanowire, from which the fine-structure splitting is predicted to vanish.³ As an additional advantage, nanowires provide a one-dimensional channel for charge transport that can be used to realize an efficient interface between the electron (or hole) spin and the polarization state of a single photon. For instance, electrons⁴ or holes⁵ confined in electrically defined quantum dots may be transferred to an optically active quantum dot within the same nanowire for the emission of a single photon.

For implementation of complex, electrically contacted devices,⁴⁻⁶ nanowires are typically transferred, lying on a substrate and emitted photons are collected from the top.⁶ There are two main problems in using this geometry. First, photon collection is inefficient because most of the emission is directed towards the higher dielectric material, i.e., the substrate. Second, photon polarization is altered by the dielectric anisotropy of the one-dimensional nanowire, which acts as a polarizer.⁷⁻¹³ As a result, photons emitted from quantum dots in nanowires with polarization aligned along the nanowire axis are more likely to be detected compared to photons polarized perpendicular to the nanowire,^{14,15} thereby destroying the original polarization information.

Here, we show an alternative scheme for excitation and light collection from nanowires lying on a substrate, which accesses the intrinsic polarization properties of the quantum emitter while simultaneously increasing the light collection efficiency. This alternative scheme is based on the excitation, and detection, via reflection on a 45°-cut micro-prism. In this letter, photoluminescence (PL) experiments of the same quantum dot from both the nanowire side and along the nanowire symmetry axis are shown and compared. Calculations of

the quantum dot angular radiation pattern for a nanowire lying on a SiO₂/Si substrate are presented that explain the 3-fold light collection enhancement via the prism compared to the typical light collection geometry of contacted nanowires.

In Fig. 1(a), we show a scanning electron microscopy (SEM) image of the micro-prism next to the silicon substrate covered by 285 nm of silicon dioxide (SiO₂) where nanowires are dispersed. Fig. 1(b) shows a higher magnification SEM image to visualize the nanowires measured in this work (NW1 and NW2) at a distance of approximately 20 μm from the substrate edge. A field of gold markers is used to select pre-characterized nanowires on the sample. Next, the substrate is cut with a diamond saw aiming within 20 μm from the selected nanowires and the reflecting prism is placed in contact with the cut substrate. Optical access has been observed for nanowires positioned up to a distance of 30 μm from the edge of the sample. In this work, we investigate InP nanowires containing a single InAsP quantum dot in the middle. Quantum dots have a typical diameter of 20 nm

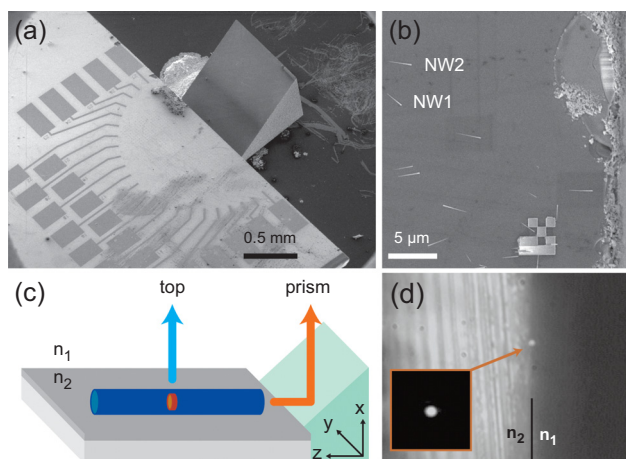


FIG. 1. (a) SEM of the 45°-cut micro-prism positioned in the vicinity of nanowires. (b) SEM of nanowires is located within ~20 μm from the edge of the sample. (c) Schematics of the two excitation and detection geometries: from the top or via reflection on the prism along the z axis. (d) White light reflection image and nanowire photoluminescence obtained via the prism. Inset shows the nanowire emission with white light off.

^{a)}Electronic address: g.bulgarini@tudelft.nl.

and a height of 10 nm, while nanowires are approximately $3\ \mu\text{m}$ long. The quantum dot is surrounded by a thin InP shell¹⁶ to improve its optical quality, resulting in a total nanowire diameter of $\sim 60\ \text{nm}$. Photoluminescence spectroscopy of individual quantum dots is performed at 10 K using a green laser at $\lambda = 532\ \text{nm}$ focused onto a $\sim 1\ \mu\text{m}$ spot using an objective with numerical aperture (NA) of 0.75.

We investigate the PL properties (intensity and polarization) of single quantum dots from two different excitation and detection geometries as sketched in Fig. 1(c). A nanowire lies at the interface between vacuum, $n_1 = 1$, and SiO_2 , $n_2 \simeq 1.45$. A single quantum dot is embedded in the nanowire and its radiative dipole lies in the xy plane, perpendicular to the nanowire elongation axis, as determined by lifetime measurements on quantum dots in nanowire waveguides¹⁷ and corroborated by PL spectroscopy in a magnetic field.¹⁵ We can excite the quantum dot and collect the photoluminescence from either the top (i.e., the side of the nanowire) or in the z direction along the nanowire high symmetry axis via reflection on the micro-prism. In order to demonstrate how this alternative scheme works, we show in Fig. 1(d) an image collected with a charged coupled device (CCD) camera showing white light reflected from the substrate edge and, in the center of the image, the PL collected from the excited nanowire and quantum dot. In this image, the excitation laser has been filtered out.

Figs. 2(a) and 2(b) show PL spectra of a single quantum dot in NW1 excited from two different geometries. In Fig. 2(a), the quantum dot PL is collected from the nanowire side via the top of the sample. Conversely, PL is collected via the prism in Fig. 2(b). Utilizing both excitation geometries, we observe the same exciton (X) and biexciton (XX) transition energies: $1235.2\ \text{meV}$ and $1233.7\ \text{meV}$, respectively. The spectra are obtained at saturation of the exciton line and the labeling of the two peaks was confirmed through analysis of power dependent PL. We note that the laser excitation power required to reach exciton saturation via the prism is four times higher than from the top due to the different excitation geometries. Moreover, we observe similar PL intensities for NW1 in both geometries because the nanowire, and thus the dipole plane, is tilted $\sim 45^\circ$ with respect to the prism.

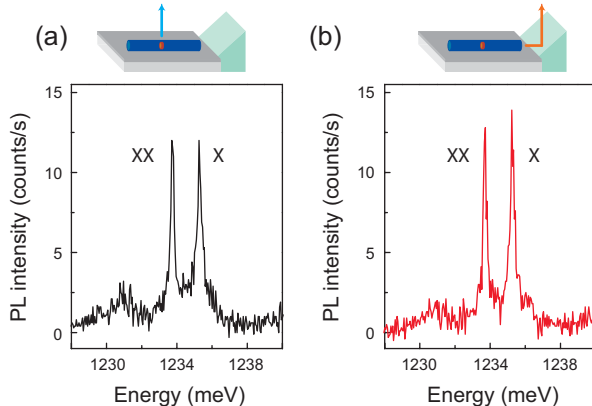


FIG. 2. Photoluminescence spectroscopy of the quantum dot in NW1 measured by using either excitation and detection from the top of the sample in (a) or via reflection of the prism in (b).

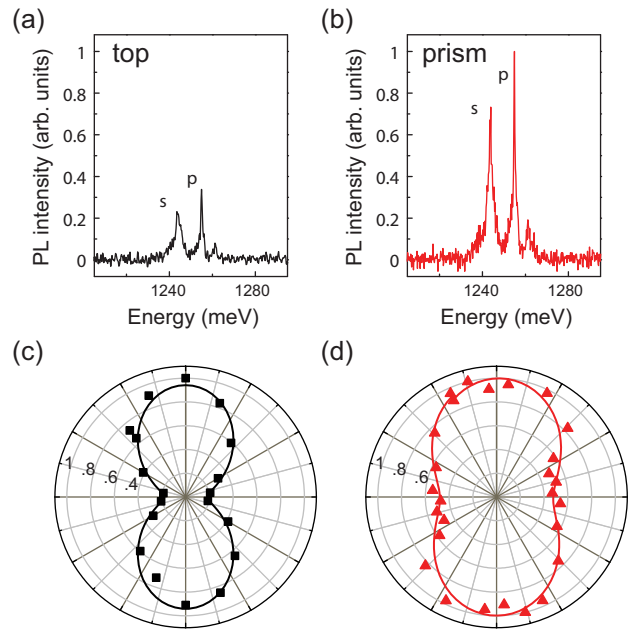


FIG. 3. (a) PL spectroscopy of the quantum dot in NW2 that is lying along the z axis, facing the prism. (b) The same quantum dot PL measured via the prism. The spectra are acquired at saturation of the s -shell and are normalized to the maximum intensity of (b). (c) Emission intensity of the s -shell measured from the top as a function of the linear polarization angle. (d) Polarization dependent PL obtained via the prism. Lines in (c) and (d) are a $\cos^2\alpha$ fit to experimental data (symbols).

In Fig. 3, we present PL spectra for NW2 that are lying along the z axis, facing the prism. In this case, the advantages of the prism collection geometry are optimally exploited. We observe a 3-fold enhancement in the PL intensity collecting via the prism (Fig. 3(b)) as compared to the top (Fig. 3(a)). The two emission peaks in Figs. 3(a) and 3(b) are attributed to the s -shell and p -shell emission of the quantum dot, acquired at saturation of the s -shell emission. In Figs. 3(c) and 3(d), we analyze the polarization properties of the quantum dot emission by using a half-waveplate followed by a polarizing beam splitter in order to detect linearly polarized emission. Importantly, we emphasize that the polarization properties of the collected light are heavily dependent on the collection geometry. First, in Fig. 3(c), the quantum dot luminescence is collected from the top of the sample. Hence, we observe a degree of linear polarization,

$$\rho = \frac{I_{\parallel} - I_{\perp}}{I_{\parallel} + I_{\perp}} \quad (1)$$

of 70%, consistent with Ref. 15. Conversely, $\rho = 35\%$ when the emission is collected by the prism in Fig. 3(d). In Eq. (1), I_{\parallel} denotes the intensity of light polarized parallel to the nanowire elongation axis, whereas I_{\perp} refers to light polarized perpendicular to it. The degree of polarization that we measure by the prism is similar to that measured on as-grown nanowires standing on the substrate ($\rho = 20\% - 30\%$).¹⁵ In that case, collected photons are emitted along the nanowire axis, similarly to what we achieve using the prism. Thus, we conclude that the intrinsic polarization properties of the quantum dot are accessed on transferred nanowires via the prism. We stress, however, that when the nanowire is not facing the

prism, as for NW1, we do not avoid the nanowire polarizing effect and we therefore observe a strong degree of linear polarization ($\sim 75\%$) using both collection geometries.

In the following, we analyze the light collection efficiency of the two methods by supporting the experimental results with calculations of the quantum dot angular radiation pattern. A single exciton confined in the quantum dot is modeled as an electric dipole lying in the xy plane, at the interface between vacuum (n_1) and SiO_2 (n_2). We model the emission pattern using the intrinsic dipole, which is constituted of a component perpendicular and a component parallel to the dielectric interface. In Fig. 4(a), we plot the emission angular distribution for $\lambda = 950$ nm in the case of a dipole aligned along x (i.e., perpendicular to the dielectric interface), and in Fig. 4(b) we plot the emission profile for a parallel oriented dipole, y direction. In both cases, we plot in the inset the emission profile of the same dipole in vacuum. As expected, most of the light is emitted by the dipole downwards, towards the higher refractive index dielectric, SiO_2 . Explicitly, the density of available photonic modes is larger in a higher refractive index material ($n_2 > n_1$) and therefore, the emitter couples light into medium 2 with higher probability than into medium 1, thus increasing the total emission rate. The anisotropy of the emission profile indicates that light collection from the top of the sample is not efficient. This effect has been measured and exploited to improve light collection from nanocrystals¹⁸ and molecules^{19,20} on transparent dielectric substrates. By increasing the n_2/n_1 ratio, the portion of photons emitted downwards can be maximized and the emission is collected from the substrate with efficiency approaching 100%.^{20,21}

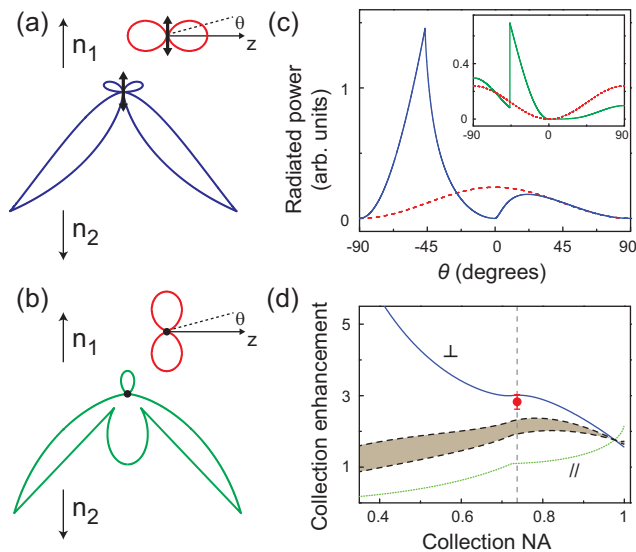


FIG. 4. Calculated angular radiation pattern for an electric dipole (double arrow) positioned perpendicular (a) or parallel (b) to the interface between vacuum (n_1) and SiO_2 ($n_2 \approx 1.45$). Insets show emission profiles in vacuum. (c) Radiated power for a dipole perpendicular to the interface (solid) compared to vacuum (dashed). Inset shows the power radiated by a parallel dipole at the interface (solid) compared to vacuum (dashed). (d) Light collection enhancement obtained via the prism instead of typical collection from the top for perpendicular (solid-blue) and parallel (dotted-green) aligned dipole. The area between dashed curves represents the expected collection enhancement taking into account both components. The dashed vertical line indicates the NA used in the experiments and the red dot represents the measured collection efficiency enhancement.

For the calculations of the radiation pattern, we have separated the quantum dot emission into two components: plane waves and evanescent waves, following the theory developed by Lukosz and Kunz.^{22,23} Plane waves propagate in vacuum and towards medium 2 with incidence angle lower than the Brewster's angle. In contrast, evanescent waves propagate from medium 1 to medium 2 at angles larger than the Brewster's angle, but with a transmission probability that depends exponentially on the distance of the dipole from the interface.^{22,23} In our calculations, we fixed the distance of the dipole from the interface to 30 nm, assuming a nanowire diameter of 60 nm and the quantum dot to be positioned on the nanowire axis.¹⁶ At this nanowire diameter, the quantum dot emission is not confined in the nanowire and only couples to the continuum of non-guided radiative modes in vacuum.^{17,24} Therefore, we neglect the nanowire dielectric in our calculations. In Fig. 4(c), we quantitatively compare the power profile of a dipole perpendicular to the vacuum– SiO_2 interface (solid line) with that of the same dipole in vacuum (dashed line). The inset shows the power emitted from a parallel dipole at the interface (solid line) compared to vacuum (dashed line). Indeed, the presence of the dielectric interface modifies the dipole emission. The total power radiated by the dipole at the interface is approximately double compared to vacuum and over 80% of the total emission is directed downwards.

We now estimate the ratio of photons that are collected via the prism versus photons collected from the top. We plot in Fig. 4(d) the collection efficiency enhancement obtained by utilizing the prism compared to collection from the top as a function of the NA of the collection optics. The solid-blue (dotted-green) curve refers to a dipole aligned along x (y), which is perpendicular (parallel) to the dielectric interface. The calculations account for a quantum dot positioned at $20 \mu\text{m}$ from the edge of the substrate, considering first-order reflections at the SiO_2/Si substrate, absorption losses in the substrate, and reflections at the sample-air interface. The calculated curve for a perpendicular dipole evidences a factor of 3 enhancement using $\text{NA} = 0.75$, whereas a lower enhancement of 1.1 is expected for a parallel dipole since there is also a strong component of emission directed normal to the dielectric interface. The grey area between black-dashed lines indicates the collection enhancement expected for the sum of perpendicular and parallel components, taking into account the intrinsic polarization anisotropy of the emitter.¹⁵ Our model qualitatively explains the measured collection efficiency enhancement of 2.9 (red dot) obtained by using the prism instead of collection from the top of the sample.

We have demonstrated that a single quantum dot embedded in a nanowire can be optically addressed from perpendicular orientations: either the top of the sample or via a micro-prism. We obtain a 3-fold improvement in light collection efficiency from lying nanowires using the prism as compared to usual detection from the top of the sample. The micro-prism collection technique is also compatible with nanowire waveguides¹⁶ to further increase the light collected from transferred nanowire devices in future work. Notably, with this excitation geometry, we access the intrinsic polarization information of the quantum emitter, thus circumventing the issue of the polarizing effect in nanowires. This achievement is of

major importance for the generation of polarization-entangled photon pairs from nanowires lying on a substrate,⁶ or for spin to photon polarization transfer of quantum information. Additionally, both excitation geometries may be utilized concurrently for resonant excitation of a single quantum dot.²⁵ Explicitly, the combination of quantum dot excitation from the top with luminescence collection via the prism would provide an on-chip solution to the issue of rejecting the resonant excitation laser. Finally, this dual excitation geometry may be employed for the study of the valence band heavy hole–light hole character^{26,27} of a quantum dot by excitation and detection along different orientations.

The authors acknowledge E. P. A. M. Bakkers for the nanowire quantum dot samples, V. E. Calado for the help provided in the sample preparation and L. Robledo for scientific discussions. This work was supported by the Netherlands Organization for Scientific Research (NWO), Dutch Organization for Fundamental Research on Matter (FOM), European Research Council, and DARPA QUEST Grant.

¹N. Gisin, G. Ribordy, W. Tittel, and H. Zbinden, *Rev. Mod. Phys.* **74**, 145–195 (2002).

²N. Gisin and R. Thew, *Nature Photon.* **1**, 165–171 (2007).

³R. Singh and G. Bester, *Phys. Rev. Lett.* **103**, 063601 (2009).

⁴S. Nadj-Perge, S. M. Frolov, E. P. A. M. Bakkers, and L. P. Kouwenhoven, *Nature* **468**, 1084–1087 (2010).

⁵Y. Hu, F. Kuemmeth, C. M. Lieber, and C. M. Marcus, *Nat. Nanotechnol.* **7**, 47–50 (2012).

⁶M. E. Reimer, M. P. van Kouwen, A. W. Hidma, M. H. M. van Weert, E. P. A. M. Bakkers, L. P. Kouwenhoven, and V. Zwiller, *Nano Lett.* **11**, 645–650 (2011).

⁷J. Wang, M. S. Gudiksen, X. Duan, Y. Cui, and C. M. Lieber, *Science* **293**, 1455–1457 (2001).

⁸H. Pettersson, J. Trägårdh, A. I. Persson, L. Landin, D. Hessman, and L. Samuelson, *Nano Lett.* **6**, 229–232 (2006).

⁹A. Lan, J. Giblin, V. Protasenko, and M. Kuno, *Appl. Phys. Lett.* **92**, 183110 (2008).

¹⁰S. Thunich, L. Prechtel, D. Spirkoska, G. Abstreiter, A. Fontcuberta i Morral, and A. W. Holleitner, *Appl. Phys. Lett.* **95**, 083111 (2009).

¹¹M. P. van Kouwen, M. H. M. van Weert, M. E. Reimer, N. Akopian, U. Perinetti, R. E. Algra, E. P. A. M. Bakkers, L. P. Kouwenhoven, and V. Zwiller, *Appl. Phys. Lett.* **97**, 113108 (2010).

¹²D. Spirkoska, A. L. Efros, W. R. L. Lambrecht, T. Cheiwchanchamnangij, A. Fontcuberta i Morral, and G. Abstreiter, *Phys. Rev. B* **85**, 045309 (2012).

¹³G. Bulgarini, M. E. Reimer, M. Hocevar, E. P. A. M. Bakkers, L. P. Kouwenhoven, and V. Zwiller, *Nature Photon.* **6**, 455–458 (2012).

¹⁴A. Tribu, G. Sallen, T. Aichele, R. André, J.-P. Poizat, C. Bougerol, S. Tatarenko, and K. Kheng, *Nano Lett.* **8**, 4326–4329 (2008).

¹⁵M. H. M. van Weert, N. Akopian, F. Kelkensberg, U. Perinetti, M. P. van Kouwen, J. Gomez Rivas, M. T. Borgström, R. E. Algra, M. A. Verheijen, E. P. A. M. Bakkers, L. P. Kouwenhoven, and V. Zwiller, *Small* **5**, 2134–2138 (2009).

¹⁶M. E. Reimer, G. Bulgarini, N. Akopian, M. Hocevar, M. Bouwes Bavinck, M. A. Verheijen, E. P. A. M. Bakkers, L. P. Kouwenhoven, and V. Zwiller, *Nat. Commun.* **3**, 737 (2012).

¹⁷G. Bulgarini, M. E. Reimer, T. Zehender, M. Hocevar, E. P. A. M. Bakkers, L. P. Kouwenhoven, and V. Zwiller, *Appl. Phys. Lett.* **100**, 121106 (2012).

¹⁸X. Brokmann, E. Giacobino, M. Dahan, and J. P. Hermier, *Appl. Phys. Lett.* **85**, 712–714 (2004).

¹⁹L. Luan, P. R. Sievert, B. Watkins, W. Mu, Z. Hong, and J. B. Ketterson, *Appl. Phys. Lett.* **89**, 031119 (2006).

²⁰K. G. Lee, X. W. Chen, H. Eghlidi, P. Kukura, R. Lettow, A. Renn, V. Sandoghdar, and S. Götzinger, *Nature Photon.* **5**, 166–169 (2011).

²¹X.-W. Chen, S. Götzinger, and V. Sandoghdar, *Opt. Lett.* **36**, 3545–3547 (2011).

²²W. Lukosz and R. E. Kunz, *J. Opt. Soc. Am.* **67**, 1615–1619 (1977).

²³W. Lukosz, *J. Opt. Soc. Am.* **69**, 1495–1503 (1979).

²⁴J. Bleuse, J. Claudon, M. Creasey, N. S. Malik, J.-M. Gérard, I. Maksymov, J.-P. Hugonin, and P. Lalanne, *Phys. Rev. Lett.* **106**, 103601 (2011).

²⁵A. N. Vamivakas, C.-Y. Lu, C. Matthiesen, Y. Zhao, S. Fält, A. Badolato, and M. Atatüre, *Nature* **467**, 297–300 (2010).

²⁶R. Vrijen and E. Yablonovitch, *Physica E (Amsterdam)* **10**, 569–575 (2001).

²⁷H. Kosaka, *J. Appl. Phys.* **109**, 102414 (2011).